Catal Lett (2017) 147:2893–2900
DOI 10.1007/s10562-017-2182-6

Effect of SO_2 on Catalytic CO Oxidation Over Nano-Structured, Mesoporous Au/$Ce_{1-x}Zr_xO_2$ Catalysts

Dolly Valechha[1] · Suresh Kumar Megarajan[2] · Anis Hamza Fakeeha[3] · Ahmed S. AL-Fatesh[3] · Nitin K. Labhasetwar[1]

Received: 23 May 2017 / Accepted: 25 August 2017 / Published online: 7 September 2017

Abstract A series of nano-structured, mesoporous Au/$Ce_{1-x}Zr_xO_2$ type catalysts were synthesized by first synthesizing $Ce_{1-x}Zr_xO_2$ type of support with different degree of Zr substitutions and following sol–gel route. One weight percent of Au was incorporated on these supports using deposition–precipitation method. These synthesized catalysts were characterized in detail by various techniques, and evaluated for their CO oxidation activity. Effect of SO_2 poisoning on catalytic CO oxidation activity was also investigated in detail. It was observed that the catalytic activity for CO oxidation reaction depends on the Ce/Zr molar ratio. The effect of SO_2 on CO oxidation was less prominent for the Zr incorporated 'Au/$Ce_{0.8}Zr_{0.2}O_2$ (ACZ0.2)' as compared to bare 'Au/CeO_2 (AC)' catalyst. In case of ACZ0.2, the activity remains quite stable even after 5 h of SO_2 exposure, however, after 12 and 18 h, the activity decreases to 62 and 55%, respectively. Whereas AC catalyst shows rapid decline in catalytic activity from the first hour of SO_2 exposure, and continue to decline significantly to 35 and 18% after 12 and 18 h of SO_2 exposure, respectively. Multiple regeneration studies of both bare and Zr incorporated catalysts show pronounced improvement/regain in catalytic activity.

✉ Nitin K. Labhasetwar
nk_labhsetwar@neeri.res.in

[1] Energy & Resource Management Division, CSIR-National Environmental Engineering Research Institute (CSIR-NEERI), Nehru Marg, Nagpur 440020, India

[2] Key Laboratory of Biobased Materials, Qingdao Institute of Bioenergy and Bioprocess Technology, Chinese Academy of Sciences, No.189 Songling Road, Qingdao 266101, People's Republic of China

[3] Chemical Engineering Department, College of Engineering King Saud University, P.O. Box 800, Riyadh 11421, Kingdom of Saudi Arabia

Graphical Abstract

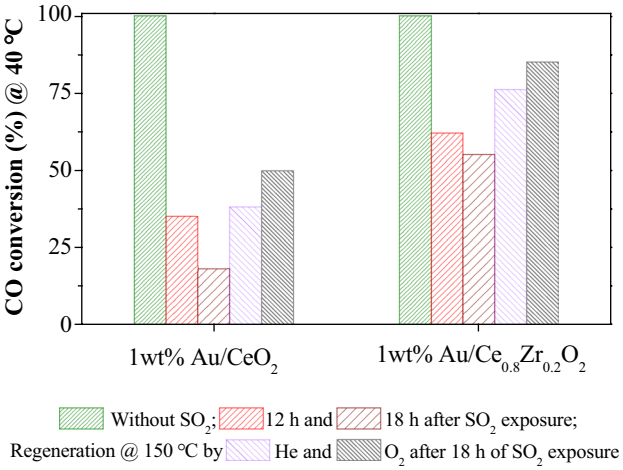

Keywords CO oxidation · Gold nano particles · Mixed metal oxide · Catalyst · Au/$Ce_{1-x}Zr_xO_2$

1 Introduction

Carbon monoxide (CO) is one of the major air pollutants released from both natural and anthropogenic sources, especially from industries, automobiles and several other combustion sources. Incomplete combustion of fossil fuels and biomass leads to CO emissions via line and point sources, such as engines, oil burners, boilers, and water heaters [1–5]. Since CO is present with different co-existing gases such as N_2, CO_2, water vapor, and sometimes including poisonous gases like SO_2 as well as at different temperatures, hence CO mitigation needs to be source specific. Catalytic CO oxidation is a well-known and commercially exploited process; however, nano-structured catalysis had opened a new

gateway for the researchers to further improve the catalysts with respect to efficiency and stability for low temperature CO oxidation. Activity of a catalyst depends on both intrinsic and physical properties, while extensive efforts have also been focused on tailoring the surface area, pore size, morphology, and other physical properties [6–13].

Haruta et al. demonstrated that supported gold nano particles are highly effective for low temperature CO oxidation reactions and they have also discussed the effect of different supports over catalytic activity [14, 15]. Catalytic activity of gold nanoparticles supported catalysts have been extensively studied using various supports such as Fe_2O_3, CeO_2, MnO_2, MgO, TiO_2, Al_2O_3, ZnO, Co_3O_4, ZrO_2, SiO_2, MCM-48, CuO–CeO_2, TiO_2–SiO_2, etc. [16–27]. Bulk gold particles are either inactive or poorly active at low temperature compared to supported gold catalysts. Exceptional activity of supported gold catalysts can be attributed to the metal-support interface as well as reducible active supports. It is generally accepted that the synergy between metal catalysts and oxide based supports, as well as reducibility of such oxide supports are significant aspects governing catalytic activity for many important reactions, including CO, VOCs, and soot oxidation [28–30]. Oxide supports are mainly categorized as active or 'reducible' and inert or 'non-reducible' support according to their redox properties. For instance, Al_2O_3, MgO, SiO_2, etc. are generally non-reducible supports while CeO_2, Fe_2O_3, MnO_2, TiO_2, etc are considered reducible or active supports because of the presence of mobile oxygen atoms. Reducible active supports enhance the oxygen mobility during the reaction, which is considered as an important criterion for oxidative reactions. As a result, developing low-cost gold catalysts with superior oxidation activity at low temperatures is still a strong area of research interest.

CeO_2–ZrO_2 mixed oxides have been widely investigated for the three-way catalysis due to their high thermal and chemical stability, these have also been found suitable for water gas shift reactions [31–33]. CeO_2–ZrO_2 based oxide catalysts are found to be more promising due to the presence of defects formed via substitution of the smaller Zr^{4+} in place of Ce^{4+} cation into the ceria lattice [34, 35]. The catalytic activity of CeO_2–ZrO_2 oxide also depends on its surface area, particle size and most importantly on Ce/Zr molar ratio [36–40]. Although catalytic CO oxidation over CeO_2–ZrO_2 supported catalysts have been studied extensively, the effect of SO_2 poisoning and regeneration studies were seldom reported [41–43]. Deshmukh et al. have studied the effect of SO_2 poisoning over CeO_2 and CeO_2–ZrO_2, and observed the superior tolerance of CeO_2–ZrO_2 in comparison with CeO_2 [41]. Two weight percent of Pd loaded (Ce–Zr) O_2 catalysts have been reported for CO oxidation by Ryou et al. although, they have observed good activity even after SO_2 exposure and regeneration, the CO conversion was achieved at the temperature below 100 °C was insignificant [43]. Therefore, it is indeed very important to develop a catalyst, which is active at lower temperatures at possibly around room temperature with different feed stream conditions. In the present study, a series of Au/$Ce_{1-x}Zr_xO_2$ were synthesized by sol gel method, and were evaluated for their catalytic activity toward CO oxidation. The effect of presence of SO_2 in the feed stream has been investigated thoroughly as a function of time-on-stream (TOS). Multiple regeneration studies have also been studied on the select catalysts using different conditions. The aim of this research is to understand the importance of physical as well as chemical properties of CeO_2 with Zr incorporation for their catalytic activity. The synthesized catalysts were characterized by using different techniques, such as Powder X-ray diffraction (*p*-XRD), transmission electron microscopy (TEM) and N_2 physisorption analysis.

2 Experimental

2.1 Materials

Cerium nitrate, zirconyl nitrate, and citric acid used for the synthesis of $Ce_{1-x}Zr_xO_2$ were procured from HiMedia, India (analytical grade). Analytical grade $HAuCl_4$ and NaOH were procured from Sigma-Aldrich and Merck India, respectively.

2.2 Synthesis of $Ce_{1-x}Zr_xO_2$ Support

The citrate sol–gel method was used for the synthesis of a series of $Ce_{1-x}Zr_xO_2$ (x = 0, 0.1, 0.2, 0.25, 0.4 and 0.5) supports. Stoichiometric amount of cerium nitrate, zirconyl nitrate, and citric acid were dissolved in requisite volume of distilled water to obtain a transparent solution (the molar ratio of total metal nitrate precursors/citric acid was kept as 1:2). The solution was gradually heated at 80 °C (around 2–3 h) to form a viscous solution or gel, and the gel was subsequently heated until a spongy mass was obtained. The spongy mass was thoroughly homogenized by grinding and subsequently calcined at 400 °C for 5 h in a muffle furnace to obtain $Ce_{1-x}Zr_xO_2$ supports.

2.3 Synthesis of Au/$Ce_{1-x}Zr_xO_2$

One weight percent of Au deposited $Ce_{1-x}Zr_xO_2$ samples were prepared by following the deposition precipitation (DP) method. Appropriate amount of the calcined $Ce_{1-x}Zr_xO_2$ powder was soaked with distilled water, and the pH of the obtained suspension was adjusted to eight by adding 0.1 M NaOH. $HAuCl_4$ solution having pH 8 (adjusted by 0.1 M NaOH solution) was added to the above suspension with continuous stirring. The mixture was stirred at 60 °C for 2 h followed by sonication for 30 min. The product thus obtained was filtered

and washed with distilled water for several times to eliminate Cl^- ions completely and subsequently dried at 110 °C for 10 h. The Au deposited $Ce_{1-x}Zr_xO_2$ samples were denoted as ACZx (x = 0.1, 0.2, 0.25, 0.4 and 0.5, where x indicates the mol% of Zr) and AC for x = 0.

2.4 Material Characterization

p-XRD patterns were recorded using Rigaku Miniflex II instrument operated at 30 kV and 15 mA with a monochromator using Cu Kα radiations. The samples were scanned in the 2θ range 10°–80° with a scanning speed of 3° min^{-1}. Diffraction peaks were compared with the standard Joint Committee on Powder Diffraction Standards (JCPDS) database reported by the International Centre for Diffraction Data (ICDD). Crystallite size was also calculated using the Scherrer's equation. N_2 adsorption–desorption isotherms were recorded at −196 °C using a Micromeritics ASAP-2000 instrument. Prior to analysis, the samples were evacuated and pretreated at 200 °C for 6 h. The pore size distribution and surface area were analyzed using the Barrett–Joyner–Halenda (BJH) and Brunauer–Emmett–Teller (BET) method, respectively.

The morphological and structural details of the select ACZ0.2 were studied by TEM. TEM was carried out on a JEOL JEM-3010 microscope operated at 300 kV (LaB_6 cathode, point resolution 1.7 Å). For TEM analysis, pinch of catalyst was dispersed in ethanol and ultrasonicated for 15 min. The suspension so obtained was dried at room temperature on a copper grid. Au loading was determined by inductively coupled plasma optical emission spectrometer (ICP–OES) using a Perkin Elmer-Optima 4100 DV instrument.

2.5 Catalytic Activity Measurements

The steady state gas evaluation assembly equipped with a quartz fixed bed type reactor, precise mass flow controllers (Alborg, USA), gas mixing chamber, heating system and gas chromatograph (GC) was used to carry out the CO oxidation reaction at atmospheric pressure. All the catalytic activity experiments were performed using 100 mg of catalysts. The simulated gas consist of 500 ppm CO, 20% O_2 balance by He with a total flow rate of 100 SCCM. The reaction was continuously analyzed online by using a Shimadzu GC (GC-2014) equipped with a thermal conductivity detector (TCD). Prior to the evaluations, all the catalysts were subjected to heat treatment in He flow at 100 °C for a period of 0.5 h, to remove any adsorbed gases or contaminant. Effect of SO_2 on catalytic CO oxidation was studied by introducing SO_2 (10–80 ppm) in the feed stream along with the other gases. The catalytic activity was evaluated in terms of % conversion (X) of CO gas to CO_2 according to the below Eq. (1),

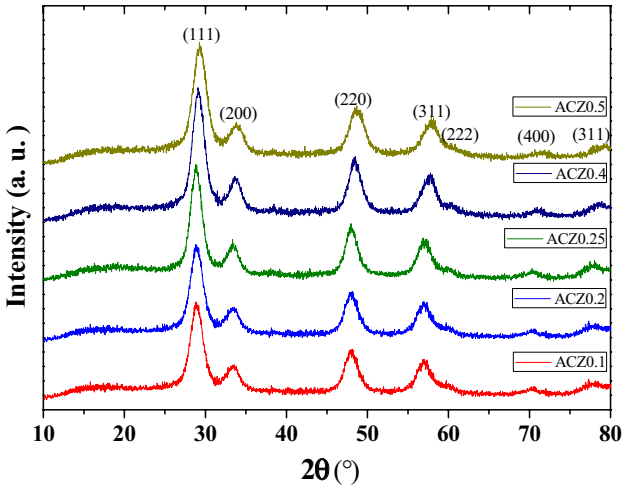

Fig. 1 *p*-XRD patterns for various ACZx (x = 0.1, 0.2, 0.25, 0.4 and 0.5) catalysts

Table 1 Structural properties of ACZx (x = 0, 0.1, 0.2, 0.25, 0.4 and 0.5) catalysts by *p*-XRD analysis

Catalysts	Lattice type[a]	t[b] (nm)	*a*[c] (Å)	*V*[d] (Å)^3
AC	CeO_2 (043-1002)	16.5	5.403	157
ACZ0.1	CeO_2 (043-1002)	16.2	5.402	157
ACZ0.2	CeO_2 (043-1002)	10.2	5.369	154
ACZ0.25	$Ce_{0.75}Zr_{0.25}O_2$ (028-0271)	8.7	5.359	153
ACZ0.4	$Zr_{0.4}Ce_{0.6}O_2$ (038-1439)	9.5	5.307	149
ACZ0.5	$Zr_{0.5}Ce_{0.5}O_2$ (038-1439)	7.8	5.306	149

[a]Reference JCPDS card number given in parenthesis

[b]Crystallite size

[c]Lattice parameter

[d]Lattice volume

$$X(CO) = \frac{F_{CO}^{in} - F_{CO}^{out}}{F_{CO}^{in}} \times 100\% \quad (1)$$

3 Results and Discussion

3.1 Characterization Studies

p-XRD analysis results of all the ACZx catalytic materials are given in Fig. 1 and Table 1. Diffraction patterns of all the samples were compared with the standard JCPDS database, which clearly confirms the formation of crystalline cubic fluorite structure (Fm3m space group) of $CeO_2/Ce_{1-x}Zr_xO_2$ solid solutions with characteristic diffraction peaks corresponding to (111), (200), (220), (311), (222), (400), and (331) planes. The gradual shift of diffraction peaks towards higher 2θ values as well as change in lattice parameters was observed with increasing Zr incorporation. Peak shift as well

as change in lattice parameters of cubic structure could be owing to the dissimilar ionic radii of Ce^{4+} and Zr^{4+} ions. No characteristic diffraction peak was observed for ZrO_2 phase with Zr incorporation up to 50% i.e., ACZ0.5, which evidently confirms the formation of CeO_2–ZrO_2 solid solutions [44, 45]. In addition, no characteristic diffraction peaks were observed for Au, mainly due to its lower content and high dispersion. The average crystallite size was calculated from line broadening of (111) plane using Scherrer's equation. The values of lattice parameter, lattice cell volume, and crystallite size are given in Table 1. Decrease in the crystallite size was observed with increase in the Zr/Ce mole ratio. The lattice constant and lattice volume of catalyst also decreases with the increase in Zr/Ce mole ratio. This suggests that unit cell of the cubic phase shrinks in the order AC > ACZ0.1 > ACZ0.2 > ACZ0.25 > ACZ0.4 > ACZ0.5, due to the substitution of smaller Zr^{4+} ion (0.84 Å) with larger Ce^{4+} ion (0.97 Å). As given in Table 2, the actual Au content on all ACZx catalysts is found to be almost close to 1% as calculated by ICP–OES analysis.

Table 2 Physical and chemical properties of ACZx (x = 0, 0.1, 0.2, 0.25, 0.4 and 0.5) catalysts

Catalysts	BET-SA ($m^2\ g^{-1}$)	Pore volume ($cm^3\ g^{-1}$)	Pore diameter (nm)	Au content (wt%)
AC	64	0.201	12.16	1.2
ACZ0.1	62	0.181	11.72	1.12
ACZ0.2	82	0.109	5.3	1.10
ACZ0.25	64	0.097	5.29	1.13
ACZ0.4	61	0.068	4.48	1.01
ACZ0.5	80	0.070	3.61	0.98

As shown in Fig. 2, the N_2 adsorption—desorption isotherms observed for AC and all ACZx catalysts were type IV indicating the presence of mesopores nature of the structure. However, the area under hysteresis curve in isotherm, as well as pore volume decreases with increasing Zr incorporation. The specific surface area, average pore size, and pore volume were also measured using N_2 adsorption isotherms as shown in Table 2. No significant change in surface area was observed with Zr incorporation, whereas the average pore

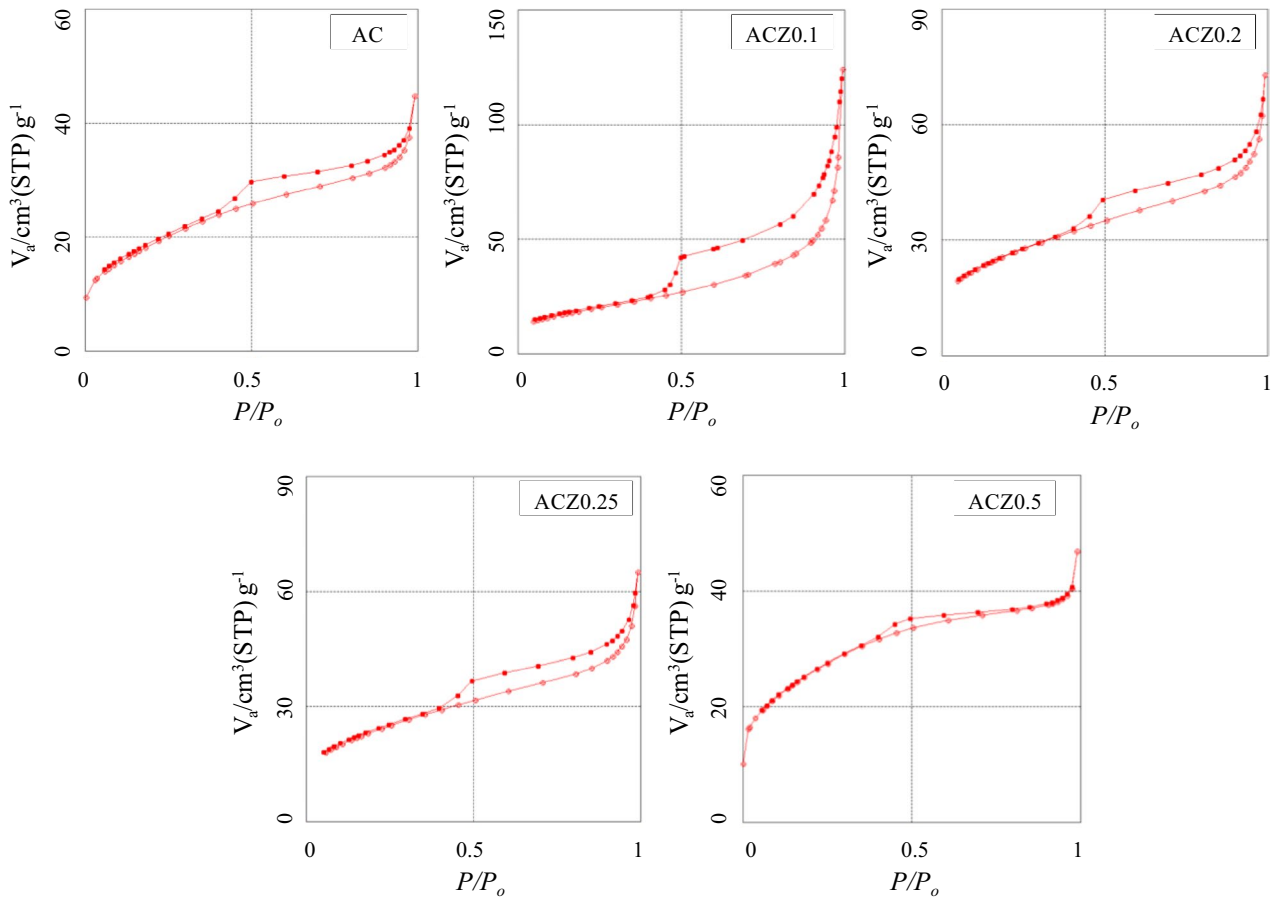

Fig. 2 Nitrogen adsorption–desorption isotherms for various ACZx (x = 0, 0.1, 0.2, 0.25 and 0.5) catalysts

Fig. 3 TEM images of ACZ0.2

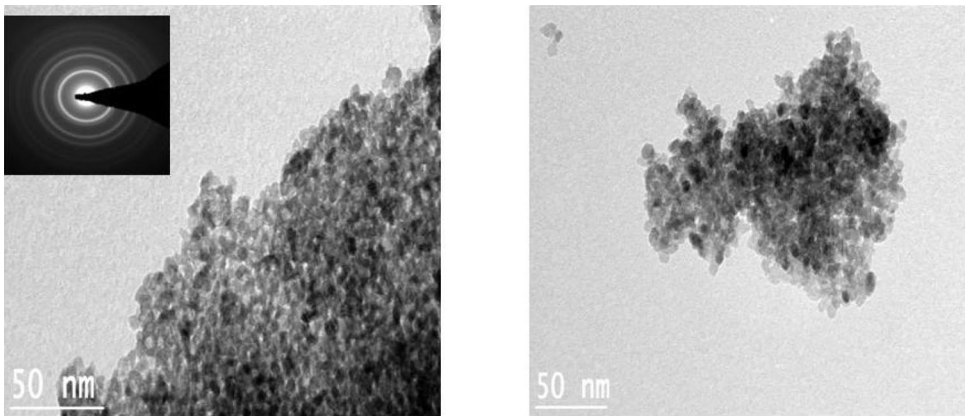

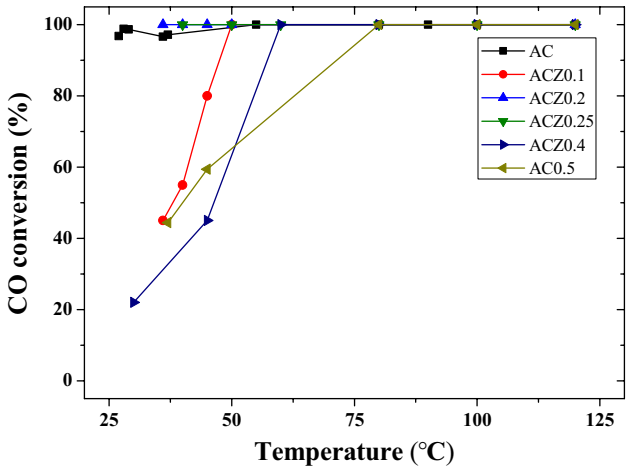

Fig. 4 CO conversion as a function of temperature for ACZx (x = 0, 0.1, 0.2, 0.25, 0.4 and 0.5) catalysts (feed: 500 ppm CO + 20% O_2, balance He; space velocity ≈ 60,000 h^{-1})

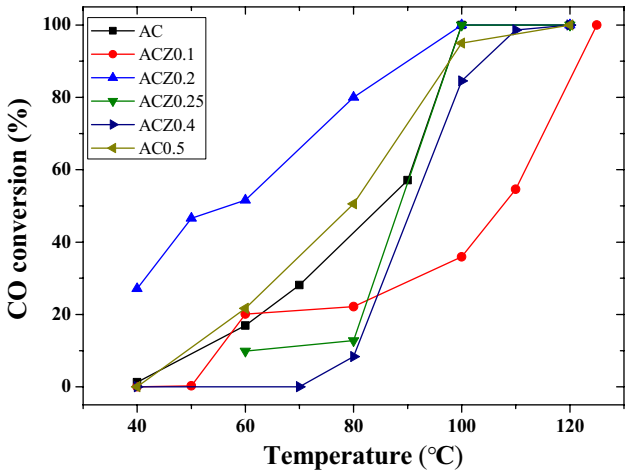

Fig. 5 Effect of SO_2 on CO conversion as a function of temperature for ACZx (x = 0, 0.1, 0.2, 0.25, 0.4 and 0.5) catalysts (feed: 500 ppm CO + 80 ppm SO_2 + 20% O_2, balance He; space velocity ≈60,000 h^{-1})

size was observed to decrease with increasing Zr component. However, the better surface area (82 m^2 g^{-1}) was observed when the Zr incorporation was 20% i.e., ACZ0.2 catalyst. The morphology and structure of the select ACZ0.2 catalyst was examined by TEM analysis as shown in Fig. 3. TEM images of ACZ0.2 display sheets of mesoporous aggregates of cubic ceria–zirconia solid solution nanocrystals. The particle size of approximately 10 nm was observed for Au nano particles. Electron diffraction pattern of ACZ0.2 catalyst as shown in inset of Fig. 3 confirms the cubic CeO_2 structure, which substantiates the result obtained by *p*-XRD.

3.2 Catalytic Activity

All the synthesized catalysts were evaluated for their catalytic activity toward CO oxidation reaction, as a function of temperature. As shown in Fig. 4, the low-temperature CO oxidation activity of AC improves with 20–25% Zr incorporation. At around 45 °C, complete CO oxidation was observed over AC catalyst, while ACZ0.2 and ACZ0.25 catalyst exhibit 100% conversion at 30 °C. However, the CO oxidation activity slightly decreases with Zr incorporation of either less or more than 20–25%. The complete CO oxidation was achieved over ACZ0.1, ACZ0.4, and ACZ0.5 at around 50, 60, and 80 °C, respectively. The overall good catalytic activity of all these Zr incorporated catalysts could be mainly because of their retained cubic phase structure, whereas the presence of tetragonal ZrO_2 phase significantly decreases the catalytic CO oxidation activity [44]. Furthermore, the light-off temperature for all the present catalysts was observed well below the room temperature even under the high space velocity conditions, which clearly explains the practical importance of these catalysts.

3.2.1 *Effect of Presence of SO_2 in the Feed on CO Oxidation*

The effect of SO_2 exposure on CO oxidation activity of AC and ACZx catalysts is presented in Fig. 5. The comparative

Table 3 T_{50}, T_{80}, and T_{100} (°C) in presence and absence of SO_2 over CO oxidation

Catalysts	Absence of SO_2[a]			Presence of SO_2[a]		
	T_{50} (°C)	T_{80} (°C)	T_{100} (°C)	T_{50} (°C)	T_{80} (°C)	T_{100} (°C)
AC	<RT[b]	<RT[b]	≈30	85	95	100
ACZ0.1	38	45	50	108	119	125
ACZ0.2	<RT[b]	<RT[b]	30	56	95	100
ACZ0.25	<RT[b]	<RT[b]	30	88	95	100
ACZ0.4	46	54	60	91	99	110
ACZ0.5	40	63	80	79	92	115

[a]Feed:500 ppm CO + 0 or 80 ppm SO_2 + 20% O_2, balance He; space velocity ≈60,000 h^{-1}

[b]Conversions achieved well below room temperature

T_{50}, T_{80}, and T_{100} with the presence and absence of SO_2 are also given in Table 3. Noticeable deterioration in CO oxidation activity was observed on all the catalysts after SO_2 introduction in the reaction gas feed. Effect of SO_2 poisoning was more prominent over AC compared to Zr incorporated ACZx catalysts at lower temperatures. In absence of SO_2, the T_{50} increases in the following order ACZ0.2 ≈ ACZ0.25 ≈ AC > ACZ0.1 > ACZ0.5 > ACZ0.4, whereas it was in the following order ACZ0.2 > AC ≥ ACZ0.25 > ACZ0.5 > ACZ0.4 > ACZ0.1 when 10 ppm SO_2 was introduced in the feed. Especially, ACZ0.2 catalyst composition was observed to be optimum with superior resistant towards SO_2 in the reaction gas feed stream at lower temperatures. However, T_{80} and T_{100} were found to be almost similar for AC and ACZ catalysts with 20–25% Zr incorporation under both the presence and absence of SO_2. Turn over frequency (TOF) was calculated as mmol of CO converted per g of catalyst per unit time. Maximum 0.02232 mmol of CO were converted per g of catalyst per min, when AC/ACZ0.2/ACZ0.25 shows the ≈100% CO conversion at room temperature, whereas ACZ0.1/ACZ0.4/ACZ0.5 converts not more than 0.01 mmol of CO at the same temperature. In presence of SO_2, the TOF was insignificant at room temperature for all the catalysts except ACZ0.2, which converts maximum of ≈0.006 mmol of CO per g of catalyst per min at room temperature. However, maximum 0.02232 mmol of CO were converted per g of catalyst per min, when AC/ACZ0.2/ACZ0.25 shows the 100% conversion at 100 °C, whereas ACZ0.1, ACZ0.4, and ACZ0.5 convert maximum of 0.008, 0.018, and 0.21 mmol of CO respectively, at 100 °C. These results clearly confirm the noticeable deterioration in CO oxidation activity observed on all the catalysts after SO_2 introduction in the reaction gas feed. However, the better TOF was observed over ACZ0.2 catalyst, compared to bare AC and other Zr incorporated catalysts at lower temperature.

3.2.2 *Catalyst Stability Studies*

The select ACZ0.2 and AC catalysts were subjected to time stream studies at 40 °C to test the catalyst stability in presence and absence of SO_2 and the results observed are shown in Fig. 6. The results for comparative activity with SO_2 exposure as a function of time and multiple regenerative studies are given in Table 4. The catalyst activity of both AC and ACZ0.2 was found to be quite stable in

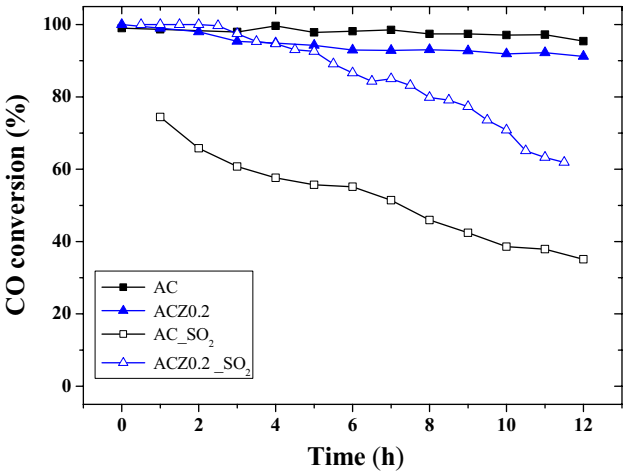

Fig. 6 Comparative catalytic stability test for AC and ACZ0.2 catalysts over CO conversion in presence and absence of SO_2 (feed: 500 ppm CO + 0 or 10 ppm SO_2 + 20% O_2, balance He; temperature: 40 °C; space velocity ≈60,000 h^{-1})

Table 4 Effect of SO_2 poisoning, and regeneration studies

Catalyst[a,b]	Initial activity[c]	Activity after 12 h poisoning	Activity after 18 h poisoning	Regeneration-1	Regeneration-2
AC	≈100	35	18	38	49.7
ACZ0.2	100	62	55	76	85
ACZ0.5	55	0	0	NP[d]	NP[d]

[a]Feed: 500 ppm CO + 0 or 10 ppm SO_2 + 20% O_2, balance He; temperature: 40 °C; space velocity ≈ 60,000 h^{-1}

[b]CO conversion values are given in percentage

[c]CO conversion values are taken just after SO_2 exposure

[d]Not performed

absence of SO_2, whereas the catalytic activity significantly deteriorates over AC as compared to ACZ0.2 catalyst with time in presence of SO_2. In case of ACZ0.2, the activity remains quite stable even after 5 h of SO_2 exposure, however, after 12 and 18 h, the activity decreases to 62 and 55%, respectively. Whereas for AC catalyst a rapid decline in catalytic activity was observed from the first hour of exposure, and continue to decline significantly with time. The activity decreases to 35 and 18% after 12 and 18 h of SO_2 exposure, respectively. The catalytic stability studies therefore, clearly substantiate the sulphur resistant over Zr incorporated catalyst [41, 43]. It was also observed that if the Zr incorporation percentage is higher SO_2 poisoning could be more susceptible. As given in Table 4, the activity of ACZ0.5 was found to be completely deteriorated, when it is subjected to longer duration SO_2 exposure. This clearly confirms that the 20% Zr incorporation would be optimum for better catalytic performance under SO_2 exposure. There are different optimal percentages of Zr incorporation on CeO_2 have been reported for better SO_2 resistance. Deshmukh et al., studied the effect of SO_2 on CeO_2 and CeO_2–ZrO_2 solid solution for CO and C_2H_6 oxidation, and reported the better SO_2 resistance over 25% Zr incorporated CeO_2 [41]. Whereas, according to Ryou et al., the better performance was achieved on 42% Zr incorporated CeO_2 catalyst, when 2 wt% Pd was dispersed on CeO_2–ZrO_2 support [43].

Decrease in catalytic activity with SO_2 exposure could be because of the adsorption of sulphur species on the catalyst surface. Therefore, multiple regeneration studies of AC and ACZ0.2 catalysts have also been performed to establish the interaction of sulphur species with the catalysts. The pronounced improvement/recovery in the catalytic activity was observed for both the catalysts as shown in Table 4. In the first regeneration step, the catalysts were heated to 150 °C for 2 h under helium flow (after 18 h of SO_2 exposure), subsequently evaluated for catalytic activity at 40 °C. After first regeneration, the catalytic activity of AC was improved from 18 to 38%, whereas it was increased from 55 to 76% over ACZ0.2. Afterwards, the catalysts were again subjected to heat treatment under O_2 flow for 2 h at 150 °C to remove any easily oxidisable species present on the catalyst surface (second regeneration). The catalysts were then cooled to 40 °C for catalytic CO oxidation test. A better improvement was observed with O_2 treatment; around 85% catalytic activity was regained over ACZ0.2 catalyst, whereas on AC catalyst 50% activity was regained. These results clearly prove that most of the sulphur species formed during reaction were present on the surface of catalysts [41], which can be easily removable via heat with air/oxygen treatment. No additional diffraction peaks for SO_2 exposed catalysts were observed in comparison with fresh catalysts by *p*-XRD analysis (not shown), which suggest that no sulfate or other sulfur bearing compound is formed under the SO_2 exposure. Only 15% catalytic activity loss was observed over ACZ0.2, while it was almost 50% loss with AC catalyst. This again validates the significance of Zr incorporation with CeO_2 for improved resistance to SO_2 and higher catalytic activity.

4 Conclusions

In conclusion, nano-structured, mesoporous Au/$Ce_{1-x}Zr_xO_2$ catalysts were successfully synthesized and subjected to CO oxidation reaction. The CO oxidation activity of Zr incorporated catalysts was found to be dependent on Ce/Zr molar ratio. ACZ0.2 catalyst exhibited the superior catalytic activity compared to bare AC catalyst in presence of SO_2 in the feed stream. AC catalyst shows rapid decline in catalytic activity from the first hour of SO_2 exposure, and continue to decline significantly to 35 and 18% after 12 and 18 h of SO_2 exposures, respectively. Whereas ACZ0.2 shows quite stable activity even after 5 h of SO_2 exposure, however, after 12 and 18 h, the activity decreases to 62 and 55%, respectively. These results clearly confirm the sulphur resistance of Zr incorporated catalyst. Catalyst regeneration by heat treatment under O_2 atmosphere results in significant improvement/regain of suppressed catalytic activity. After regeneration, merely 15% catalytic activity loss was observed over ACZ0.2, while it was almost 50% loss with AC catalyst. This again confirms the significance of Zr incorporation with CeO_2 for improved activity. Regeneration studies also reveal that the interaction between sulphur species and the catalyst was only suprafacial. In this way it appears that Au nano-particles based CO oxidation catalysts shows potential for their practical applications if improved support materials are used.

Acknowledgements This research work was carried out under the International Scientific Partnership Programme (through ISPP#0057) of King Saud University, Riyadh, Saudi Arabia for establishing research collaboration between King Saud University and CSIR-NEERI. Thanks are also due to Director CSIR-NEERI for providing research facilities. KRC no-811268512.

References

1. Seyfi B, Baghalha M, Kazemian H (2009) Chem Eng J 148:306–311
2. Morikawa A, Suzuki T, Kanazawa T et al (2008) Appl Catal B Environ 78:210–221
3. Morikawa A, Kikuta K, Suda A, Shinjo H (2009) Appl Catal B Environ 88:542–549
4. Zhang J, Smith KR, Uma R et al (1999) Chemosph Glob Chang Sci 1:353–366
5. Olivier JGJ, Pieter J, Bloos J et al (1999) Chemosph Glob Chang Sci 1:1–17

6. Cuenya BR (2010) Thin Solid Films 518:3127–3150
7. Royer S, Duprez D (2011) ChemCatChem 3:24–65
8. Min BK, Friend CM (2007) Chem Rev 107:2709–2724
9. Lu J, Zhang Y, Jiao C et al (2015) Sci Bull 60:1108–1113
10. Miceli P, Bensaid S, Russo N, Fino D (2014) Nanoscale Res Lett 9:254
11. Santillo G, Deorsola FA, Bensaid S et al (2012) Chem Eng J 207:322–328
12. Megarajan SK, Rayalu S, Nishibori M, Labhsetwar N (2015) New J Chem 39:2342–2348
13. Megarajan SK, Rayalu S, Nishibori M et al (2015) ACS Catal 5:301–309
14. Haruta M, Kobayashi T, Sano H, Yamada N (1987) Chem Lett 405–408
15. Haruta M, Yamada N, Kobayashi T, Iijima S (1989) J Catal 115:301–309
16. Pillai UR, Deevi S (2006) Appl Catal A Gen 299:266–273
17. Pattrick G, Van Der Lingen E, Corti CW et al (2004) Top Catal 30/31:273–279
18. Wu KC, Tung YL, Chen YL, Chen YW (2004) Appl Catal B Environ 53:111–116
19. Bandyopadhyay M, Korsak O, Van Den Berg MWE et al (2006) Microporous Mesoporous Mater 89:158–163
20. Bond GC, Thompson DT (2000) Gold Bull 33:41–50
21. Qian K, Jiang Z, Huang W (2007) J Mol Catal A Chem 264:26–32
22. Menard LD, Xu F, Nuzzo RG, Yang JC (2006) J Catal 243:64–73
23. Pandey AD, Güttel R, Leoni M et al (2010) J Phys Chem C 114:19386–19394
24. Haruta M (2003) Chem Rec 3:75–87
25. Moreau F, Bond GC, van der Linden B et al (2008) Appl Catal A Gen 347:208–215
26. Tai Y, Murakami J, Tajiri K et al (2004) Appl Catal A Gen 268:183–187
27. Haider P, Grunwaldt J-D, Seidel R, Baiker A (2007) J Catal 250:313–323
28. Piumetti M, Bensaid S, Andana T et al (2017) Appl Catal B Environ 205:455–468
29. Rodriguez JA, Liu P, Hrbek J et al (2007) Angew Chem Int Ed 46:1329–1332
30. Cargnello M, Doan-nguyen VVT, Gordon TR et al (2013) Science 341:771–774
31. Ozawa M, Okouchi T, Haneda M (2015) Catal Today 242:329–337
32. Yang X, Yang L, Lin S, Zhou R (2015) J Hazard Mater 285:182–189
33. Jeong D-W, Na H-S, Shim J-O et al (2015) Catal Sci Technol 5:3706–3713
34. Alifanti M, Baps B, Blangenois N et al (2003) Chem Mater 15:395–403
35. Madier Y, Descorme C, Le Govic AM, Duprez D (1999) J Phys Chem B 103:10999–11006
36. Dobrosz-Gómez I, Kocemba I, Rynkowski JM (2008) Appl Catal B Environ 83:240–255
37. Dobrosz-Gómez I, Gómez-García MÁRJ (2010) Kinet Catal 51:823–827
38. Mastelaro VR, Briois V, de Souza DP, Silva CL (2003) J Eur Ceram Soc 23:273–282
39. Boaro M, Vicario M, Llorca J et al (2009) Appl Catal B Environ 88:272–282
40. Letichevsky S, Tellez CA, de Avillez RR et al (2005) Appl Catal B Environ 58:203–210
41. Deshmukh SS, Zhang M, Kovalchuk VI, D'Itri JL (2003) Appl Catal B Environ 43:135–145
42. Luo T, Gorte RJ (2004) Appl Catal B Environ 53:77–85
43. Ryou Y, Lee J, Lee H et al (2015) Catal Today 258:518–524
44. Ayastuy JL, González-Marcos MP, Gil-Rodríguez A et al (2006) Catal Today 116:391–399
45. Yu JC, Zhang L, Lin J (2003) J Colloid Interface Sci 260:240–243